JACS
JOURNAL OF THE AMERICAN CHEMICAL SOCIETY
Article
pubs.acs.org/JACS

Nitrogen–Nitrogen Bonds Undermine Stability of N-Doped Graphene

Vitaly V. Chaban*[,†,‡] and Oleg V. Prezhdo[‡]

[†]Instituto de Ciência e Tecnologia, Universidade Federal de São Paulo, 12231-280, São José dos Campos, SP, Brazil
[‡]Department of Chemistry, University of Southern California, Los Angeles, California 90089, United States

Supporting Information

ABSTRACT: Two-dimensional alloys of carbon and nitrogen draw strong interest due to prospective applications in nanomechanical and optoelectronic devices. The stability of these chemical structures can vary greatly as a function of chemical composition and structure. The present study employs hybrid density functional theory and reactive molecular dynamics simulations to elucidate how many nitrogen atoms can be incorporated into the graphene sheet without destroying it. We conclude that (1) the C/N = 56:29 structure and all nitrogen-poorer structures maintain stability at 1000 K; (2) the stability suffers greatly in the presence of N–N bonds; and (3) distribution of electron density depends heavily on the structural pattern in the N-doped graphene. Our calculations support the experimental efforts aimed at production of highly N-doped graphene and generate important insights into the mechanisms of tuning graphene mechanical and optoelectronic properties. The theoretical prediction can be tested directly by chemical synthesis.

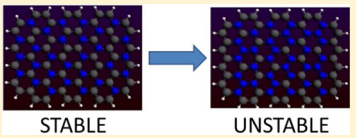

INTRODUCTION

Graphene is a carbonaceous nanomaterial with considerable scientific impact and technological promise. Research on graphene is evolving rapidly, witnessing a variety of novel synthetic approaches and many applications.[1−15] Extremely versatile chemically, carbon atoms can interact in a variety of ways. The tetrahedral arrangement of the sp^3 carbon gives diamond, while the sp^2 carbon forms layers with a hexagonal, chicken-wire structure, to produce graphite. The hexagonally arranged carbon–carbon bonds are rich in high-energy electrons. This important feature allows graphite to conduct electricity along the layers. Graphene consists of just a single layer of graphite. Various morphologies of graphene have been obtained including two-dimensional graphene nanosheets,[16] one-dimensional graphene nanoribbons,[17,18] and zero-dimensional graphene quantum dots.[19−21]

The electronic properties of graphene are substantionally different from those of other carbonaceous nanostructures, such as graphite, fullerenes, and nanotubes.[22−25] The properties of nanoribbons and quantum dots can be efficiently tuned by adjusting their size and chemical composition of edges. For instance, very narrow nanoribbons (<10 nm) exhibit semiconducting behavior, whereas wider nanoribbons exhibit very weak size dependence. The zigzag edge decreases the band gap.

Charge carriers in graphene behave in unusual ways, which originate from interactions within the symmetrical periodic arrangement of electrons spread across the hexagonal lattice. The lattice is responsible for waves of electric charge, known as quasiparticles. Retaining the quantum features of electrons (finite charge and spin), charged particles in graphene exhibit features of massless photons (linear energy–momentum dispersion relationship), requiring the special theory of relativity.[26] This opens avenues to test the relativistic theory using graphene, avoiding, to a certain extent, high-energy particle accelerators.

Graphene electronic and nanomechanical properties can be controlled by both structure and doping with other elements.[19,23,27−30] Nitrogen, boron, sulfur, and silicon can be readily incorporated into the graphene hexagonal lattice, without breaking its overall structure.[28,31] By altering the chemical, mechanical, and electrical properties of graphene, these dopants open a myriad of possibilities[23,27−30] to extend existing applications of the pure graphene and the two-dimensional boron nitride.

The N-doped graphene exhibits drastically different properties, compared to the pristine graphene.[4−14,19,23,27,28,30,31] The spin and electron density distributions for carbon atoms are influenced by neighboring nitrogen add-atoms, which create an activated region on the graphene surface. Such an activated region can catalyze or participate directly in a variety of chemical reactions. For instance, it fosters oxygen reduction and anchors metal nanoparticles used in many other catalytic processes. N-doping shifts the Fermi level above the Dirac point and opens a band gap between the conduction and valence bands. The possibility to engineer a band gap makes graphene a suitable candidate for semiconductor device applications. N-graphene draws interest in the context of sensors, batteries, and supercapacitors. N-doping of graphene greatly broadens its laboratory and industrial applications in general.[19,27,28,31]

The review of Liu et al.[32] focuses on two chemical doping approaches and band gap tuning. The review of Wang and coworkers[28] summarizes different synthetic and characterization methods of N-substituted graphene and discusses potential

Received: June 7, 2015
Published: August 27, 2015

DOI: 10.1021/jacs.5b05890
J. Am. Chem. Soc. 2015, 137, 11688–11694

Table 1. Simulated Systems, Their Properties, and Stability[a]

no.	formula	no. of electrons	stability	C/N ratio	N (%)	comments
I	$C_{74}N_{10}H_{24}$	538	stable	74:10	9.3	1 N per aromatic ring
II	$C_{64}N_{20}H_{24}$	548	stable	64:20	18.5	2 N per aromatic ring
III	$C_{51}N_{33}H_{24}$	560	unstable	51:33	30.6	3 N per aromatic ring
IV	$C_{56}N_{28}H_{24}$	556	stable	56:29	26.9	max. N without N−N bonds
V	$C_{48}N_{36}H_{24}$	564	unstable	48:36	33.3	4 N per aromatic ring

[a]The stability was identified based on the 10 ns long reactive molecular dynamics trajectories at 1000 K. Note that the percentage of nitrogen atoms is provided with respect to all atoms in the hexagonal N-doped graphene sheet. This detail is important when comparing our stability results with other experimental and theoretical investigations.

applications of N-graphene based on the existing experimental and theoretical studies. It has been reported that C_3N_4 and $C_6N_9H_3$ compositions of N-graphene feature a large band gap, ca. 5 eV.[33] The band gap can be tuned by external stress or add-atoms. In the case of the delta-doping, in which the highly concentrated dopant is confined onto a narrow region surrounded by nominally undoped graphene, the band gap is opened only when the nitrogen content exceeds 25%. It has been noted[34] that delta-doping is not a likely substitution product in real chemical practice. As a result of the chemical doping, electron−hole mobilities and conductivities become asymmetric with respect to the Dirac point of graphene. Even for a doping concentration as large as 4.0%, the conduction is marginally affected by quantum interference effects, preserving the transport properties.[35] While maintaining competitive conductivity, N-doping modulates graphene properties. Unfortunately, practical methods of graphene doping not only introduce nitrogen atoms but also create defects. Defects constitute scattering centers affecting charge mobility. When the nitrogen concentration rises above 5%, a strong localization effect may be expected, which will decrease the mobility in the N-graphene.[28]

Computer simulations constitute an efficient tool for investigating graphene structure and physical properties. Electronic structure methods are needed to determine energy levels, densities of states, band gaps, partial electrostatic charges, and excitation energies. In turn, molecular dynamics simulations, based on preparametrized potentials, account for thermal motions, entropic effects, and other nuclear properties. Significantly less computationally expensive than electronic structure calculations, classical molecular dynamics is particularly efficient in searching for the global minimum of a given nuclear-electronic system, if the corresponding statistical mechanical ensemble contains a significant number of interaction centers.

This work reports a combined simulation study employing long-time reactive molecular dynamics (RMD) simulations[36] and hybrid density functional theory (HDFT) to understand the stability of the N-doped graphene sheets as a function of their chemical composition and internal structure. We consider five different cases of N-doped graphene and test their sustainability upon thermal motion at 1000 K. N-doping creates partial electrostatic charges on every atom and modifies valence and conduction band orbitals. The electron density distribution depends strongly on the structural pattern resulting from N-doping. We conclude that nitrogen−nitrogen bonds constitute the most vulnerable structural pattern, whereas carbon−nitrogen bonds remain perfectly stable over the course of the high-temperature RMD simulations.

■ COMPUTATIONAL METHODOLOGY

The work considers five distinct systems representing different compositions of the N-doped graphene (Table 1). These particular systems are constructed to test the key alternative arrangements of the host and dopant atoms with increasing nitrogen/carbon ratios.

The molecular dynamics (MD) simulations were performed using a quantum chemistry (QC) based reactive force field (ReaxFF).[36−38] This methodology was applied previously with success to address a number of complicated problems in organic chemistry and materials science.[36−38] ReaxFF provides a nearly ab initio level of description of reactive potential surfaces for many-particle systems.[36−38] The method treats all atoms in the system as separate interaction centers. The instantaneous point charge on each atom is determined by the electrostatic field due to all surrounding charges, supplemented by the second-order description of dE/dq, where E is internal energy and q is electrostatic charge on a given atom. The interaction between two charges is written as a shielded Coulomb potential to guarantee correct behavior of covalently bonded atoms. The instantaneous valence force and interaction energy between two atoms are determined by the instantaneous bond order. The latter is determined by the instantaneous bond distance. These interaction energy functions are parametrized vs QC energy scans involving all applicable types of bond-breaking processes. The bond order concept is used to define other valence interactions, such as bond, lone electron pair, valence angle, conjugation, and torsion angle energies. It is important for energy conservation and stability that all interaction terms smoothly decay to zero during bond dissociation. The conventional pairwise van der Waals energy term describes short-range electron−electron repulsion, preserving atom size, and longer-range London attractive dispersion. Unlike nonreactive MD simulations, ReaxFF uses the van der Waals term for covalently bonded atoms, where it competes with a monotonically attractive bond term. Such an approach to chemical bonding requires a significant number of independent parameters, which can be obtained from QC energies.[36−38] Bond dissociation, geometry distortion, electrostatic charges, infrared spectra, equations of state, and condensed-phase structure are typically derived using an electronic structure method, such as density functional theory, to be consequently used in the ReaxFF parametrization. The works by van Duin, Goddard and co-workers[36−38] provide a more comprehensive description of the methodology used here. The implementation in ADF2013 (scm.com) was used for these simulations.

The HDFT calculations on the doped graphene sheets were performed using the recently proposed functional wB97xD.[39] This functional performs well for electronic structure, thermochemistry, and intermolecular binding energies. It also includes an empirical correction for dispersive attraction. Due to its good reputation, wB97xD is preferred over the more traditional HDFT approaches. Kohn−Sham orbitals were represented using the Gaussian 6-311G basis set supplemented by polarization and diffuse functions on every non-hydrogen atom, 6-311+G*. This basis set provides a reasonable balance between an affordable computational cost for a relatively large system and accuracy of electronic energy levels, partial electrostatic charges, and molecular orbitals.[39] All electrons in the systems were represented explicitly, requiring no effective-core potentials. The geometries of the N-doped graphene sheets were optimized by the conjugate gradient algorithm, prior to calculating the properties. Frequency analysis followed each geometry optimization to ensure the absence of imaginary frequency modes. The implementation in Gaussian 09, rev. D (www.gaussian.com) was used for these calculations.

DOI: 10.1021/jacs.5b05890
J. Am. Chem. Soc. 2015, 137, 11688−11694

RESULTS AND DISCUSSION

Figure 1 summarizes the initial geometries of the N-doped graphene sheets. System I features random substitution of carbon

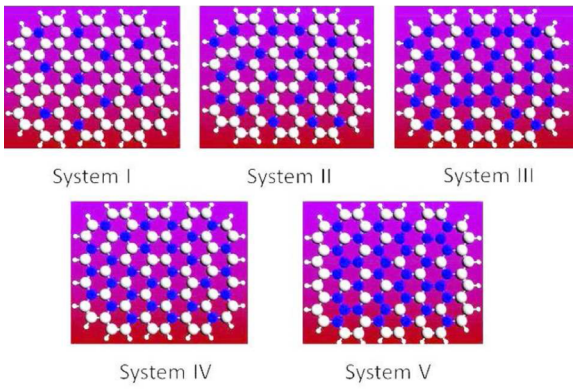

Figure 1. Initial geometries of the five investigated systems; see Table 1. Nitrogen atoms are blue, and carbon atoms are white.

atoms by nitrogen atoms under the condition that no more than a single nitrogen atom occurs per carbon ring. The same conditions are fulfilled for systems II and III, where no more than two and three nitrogen atoms per six-membered ring were allowed. System IV contains the maximum possible number of nitrogen atoms, but without any nitrogen–nitrogen bonds. Finally, system V contains four nitrogen atoms per ring. Note that nitrogen atoms are not placed at the edge; i.e., there is no nitrogen–hydrogen bond. No other constraints were applied to the structural formulas. In particular, nitrogen atoms were placed randomly subject to the above constraints.

Structural Stability. Reactive molecular dynamics simulations[37] provide an efficient and relatively inexpensive tool to observe the stability of the constructed chemical structures at finite temperature (Figures 2–3). Systems I–II appear perfectly

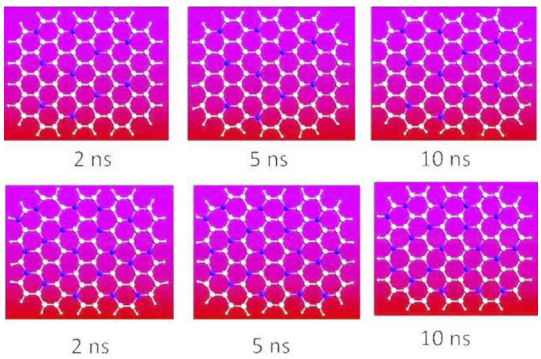

Figure 2. Atomistic snapshots taken in the course of reactive molecular dynamics for systems I (top) and II (bottom). Nitrogen atoms are blue, and carbon atoms are white.

stable during the 10 ns long RMD simulations at 1000 K. However, systems III and V are less stable. System V decomposes during the first nanosecond of the RMD simulation. System III, in turn, destructs a number of its bonds, mostly nitrogen–nitrogen bonds, but preserves a certain structure during the entire 10 ns long RMD. System IV does not contain nitrogen–nitrogen bonds, but contains 25.9% nitrogen atoms (with respect to all other atoms including hydrogen atoms). This doped structure maintains stability, in contrast to system III where many

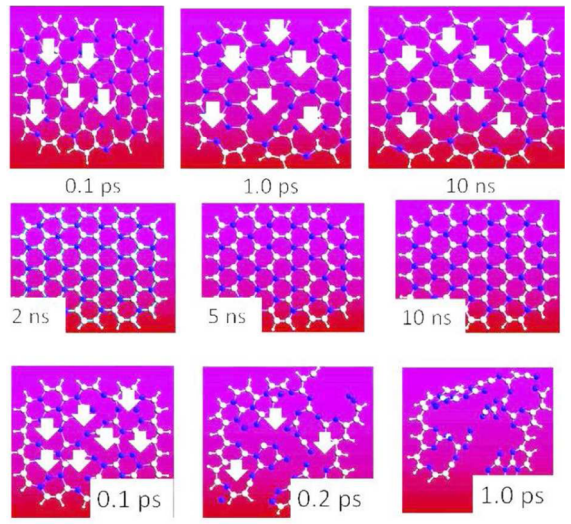

Figure 3. Atomistic snapshots taken in the course of reactive molecular dynamics for systems III (top), IV (middle), and V (bottom). Nitrogen atoms are blue, and carbon atoms are white. The white arrows point to disruptions of the N-graphene structures. N–N covalent bonds creak most often.

nitrogen–nitrogen bonds disappear readily. The local effect of nitrogen–nitrogen bonds is independent of the size of an N-doped graphene sheet.

Figures 4–7 provide a detailed description of the N-doped graphene structures in terms of the carbon–carbon, carbon–

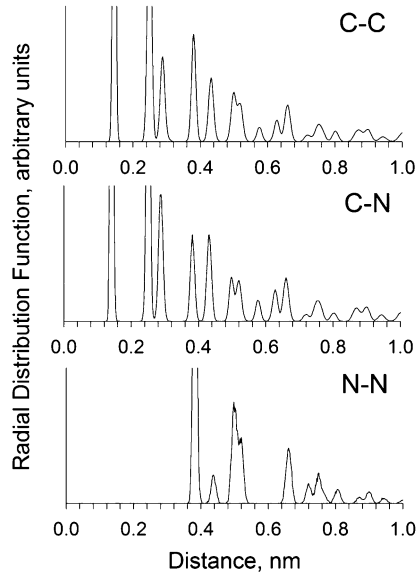

Figure 4. Radial distribution functions for the carbon–carbon, carbon–nitrogen, and nitrogen–nitrogen atomic pairs in system I; see Table 1. The functions were evaluated based on the 10 ns long reactive molecular dynamics simulation at 1000 K.

nitrogen, and nitrogen–nitrogen radial distribution functions. The carbon–carbon covalent bond length amounts to ca. 0.14 nm and fluctuates insignificantly, due to its strength and aromatic nature. This bond remains stable during molecular dynamics at 1000 K in most considered cases (Table 1). Nitrogen doping influences neither the length nor stability of this bond. Consider the multiple peaks at 0.14, 0.25, 0.29, 0.38, 0.43, 0.50, 0.52, 0.58,

DOI: 10.1021/jacs.5b05890
J. Am. Chem. Soc. 2015, 137, 11688–11694

0.63, and 0.66 nm (Figure 4, system I). Out of these, only the peak at 0.14 nm corresponds to the covalent C−C bonds, whereas all other sharp and relatively high peaks arise due to the distinct arrangement of carbon atoms in the hexagonal cells. These peaks can be used directly for interpretation of experimental X-ray data for N-doped graphene.

The carbon−nitrogen bond exhibits reasonable stability (Figures 4−7). The bond length is similar to the length of the

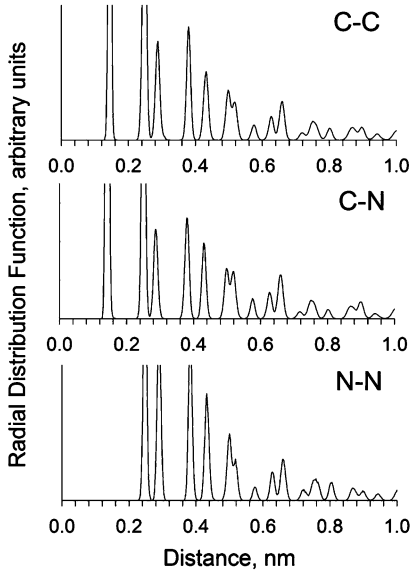

Figure 5. Radial distribution functions for the carbon−carbon, carbon−nitrogen, and nitrogen−nitrogen atomic pairs in system II; see Table 1. The functions were evaluated based on the 10 ns long reactive molecular dynamics simulation at 1000 K.

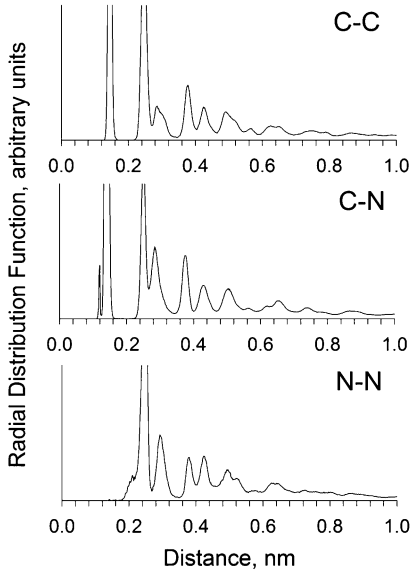

Figure 6. Radial distribution functions for the carbon−carbon, carbon−nitrogen, and nitrogen−nitrogen atomic pairs in system III; see Table 1. The functions were evaluated based on the 10 ns long reactive molecular dynamics simulation at 1000 K.

C−C covalent bond. The sharp and high peaks in the radial distribution functions (RDF) indicate that oscillations of this bond during the 1000 K equilibrium dynamics are small. Breakage of this bond is unlikely, even if the simulation of finite-

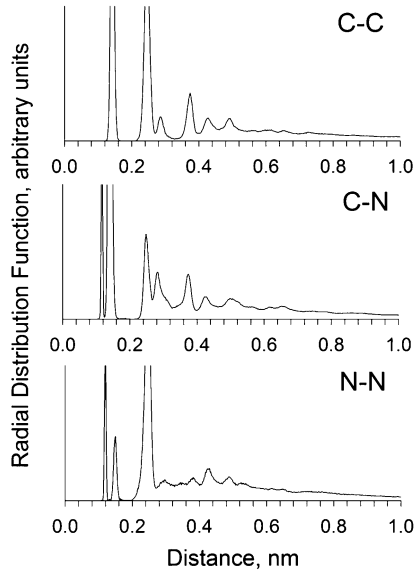

Figure 7. Radial distribution functions for the carbon−carbon, carbon−nitrogen, and nitrogen−nitrogen atomic pairs in system V; see Table 1. The functions were evaluated based on the 10 ns long reactive molecular dynamics simulation at 1000 K.

temperature dynamics is extended to greater time. Not only the covalent carbon−nitrogen distances are well-defined, but also longer (noncovalent) distances are distinguished well. Consider the peaks at 0.14, 0.25, 0.29, 0.38, 0.43, 0.50, 0.52 nm, etc. (Figure 5, system II). The discussed correlations persist during ca. 1.0 nm in the intramolecular RDFs. Note a clear similarity between the C−C and C−N peak locations. Carbon and nitrogen atoms possess nearly the same van der Waals size, which allows them to conveniently integrate into the crystalline cells of one another with minor perturbations of the overall structure. If only this point of reference is considered, graphene can be infinitely doped by nitrogen atoms. However, we know that pure nitrogen does not produce rings and thus an N-doped graphene sheet must transform into molecular nitrogen at a certain dopant concentration. The goal of the present study is to provide RMD and electronic structure evidence regarding sustainability of the N-doped graphene sheets.

In contrast to the carbon−carbon and carbon−nitrogen bonds, nitrogen−nitrogen bonds, seen in systems III and V, exhibit poorer stability and break during the first hundreds to thousands of molecular dynamics steps. While,, in system III, destruction of the N−N bonds leads to formation of the nine- and higher-membered rings (Figure 3), which remain relatively stable, system V loses its graphene-like shape very quickly. System IV preserves stability thanks to an even distribution of nitrogen atoms throughout the sheet, even though the molar fraction of the dopant in system IV is comparable to that of systems III and V. Recall that system IV has no N−N bonds, but contains many C−N bonds. Compare the RDF peaks at 0.25, 0.29, 0.38, 0.42, 0.49, and 0.64 nm (Figure 5, system III) and at 0.12, 0.15, 0.24, and 0.43 nm (Figure 7, system V). The total number of N−N RDF peaks is significantly smaller than the total number of either C−C or C−N peaks in any system. Poorly defined RDF peaks and peaks shifted to larger distances provide signs of upcoming fragmentation reactions and can be used to predict which bonds are most likely to break first.

A great advantage of RMD is its realistic description of bonded parameters (lengths, angles) and their dynamics in the course of

DOI: 10.1021/jacs.5b05890
J. Am. Chem. Soc. 2015, 137, 11688−11694

the equations-of-motion propagation. More traditional, pairwise interaction potentials oversimplify the description, which is unacceptable for the present highly precise study and for comparison with the experimental data in the case of nontrivial chemical structures.

If excess atomistic oxygen is supplied to the systems, it will foster oxidation of system V toward the CO_2, nitrogen oxides, and H_2O vapor. If oxygen is lacking, nitrogen may remain in the molecular N_2 form, depending on temperature and other reactants. At room conditions, N_2 is known to be more stable than any N_xO_y compound. Similar decomposition reactions were observed by us recently.[40] Note that the covalent N−N bonding peaks are missing in Figures 4−5 due to the initial absence of the N−N bonds in systems I and II, rather than because of N−N bond dissociation during molecular dynamics. Sharp non-covalent peaks are present in these systems, proving the integrity of the N-doped graphene sheet.

Interestingly, the marginal peak at ca. 0.17 nm (Figure 7, system V) is still present, corresponding to sporadic N−N bonds, although the molecular snapshots clearly indicate collapse of the initial structure. Furthermore, the observed N−N bond length is much longer than that of the conventional N−N bond, 0.12−0.13 nm upon high-temperature thermal motion. In contrast to the data for systems I and II (Figures 4−5), the longer-range N−N structure is absent in system V (Figure 7).

Electronic Properties. Figure 8 summarizes the valence and conduction band molecular orbitals (MOs) for the four N-doped

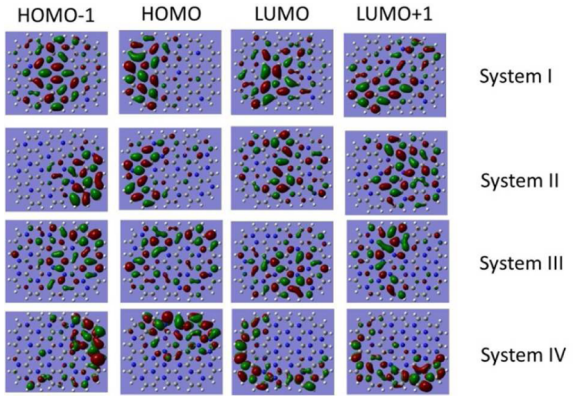

Figure 8. Visualization of the selected molecular orbitals (HOMO − 1, HOMO, LUMO, and LUMO + 1) in systems I, II, III, IV. The calculations are based on the wB97xd/6-311+G(d) level of theory. The geometries correspond to their local minima achieved by the conjugate gradient internal energy minimization algorithm. These geometries do not account for thermal motion. Note that system III, which is unstable at 1000 K, preserves its geometry at 0 K.

graphene sheets. These orbitals have been computed prior to molecular dynamics at 1000 K. They correspond to the optimized geometry configurations. System III can be optimized into a stable geometry; however, it breaks apart at 1000 K. All depicted MOs are preferentially localized on the carbon atoms, rather than on hydrogen and nitrogen atoms. The graphene sheets exhibiting less stability have somewhat more localized MOs in general, although the difference is not drastic. The highest occupied MO of the nitrogen atoms lies lower in the energy diagram than the HOMO of the sheet. We anticipate that nitrogen atoms significantly alter the valence electronic band of pristine graphene, which is the primary reason for instability of the critical dopant content.

Atomic charges on carbon, nitrogen, and hydrogen atoms supplement the outlined observations from RMD and MOs and provide an additional description of the N-doped graphene sheet instability upon use of excessive dopant. Figures 9−11 provide

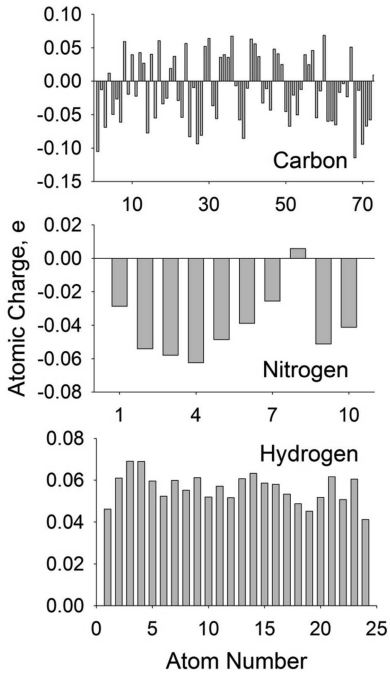

Figure 9. Atomic charges localized on carbon, nitrogen, and hydrogen atoms of system I. The charges are defined according to the Hirshfeld scheme and are given in electron units. The calculation is performed for the minimum geometry obtained at the wB97xd/6-311+G(d) level of theory. The atom numbers are the default values assigned during the computation. They do not reflect a particular order in the chemical structure.

Hirshfeld charges on every atom of systems I, III, IV. These particular systems were chosen, since they preserve stability after geometry optimization, despite N-doping. System II is omitted since its behavior is similar to that of system I. Figure 12 summarizes the observations by depicting the total charges on C, N, and H atoms in the corresponding systems. Certain similarities of all stable graphene sheets should be outlined.

First, carbon atoms attain both positive and negative electron density. The total charge on the carbon atoms in system III is nearly zero. Second, all hydrogen atoms attain a small positive charge, usually less than +0.1e. Third, all nitrogen atoms are negatively charged with only a single exception in systems I and III and no exception in system IV. Therefore, larger nitrogen content favors electron accumulation on nitrogens. Although the accumulated charges are relatively small, a systematic electron accumulation on nitrogen, instead of carbon, leads to polarization of carbon−nitrogen covalent bonds, likely making the bonds weaker. Additionally, excess electron density on both nitrogen atoms in a N−N bond makes this covalent bond particularly unstable. Accumulation of negative charge on nitrogen atoms upon their stepwise addition to the sheet is clearly seen in Figure 12.

Having conducted the RMD finite-temperature simulations, the MO analysis, and the electron-density localization analysis, we conclude that the major vulnerability of the N-doped graphene sheet is linked to the presence of the N−N bonds. The N-doped graphene sheet is stable irrespective of the nitrogen

DOI: 10.1021/jacs.5b05890
J. Am. Chem. Soc. 2015, 137, 11688−11694

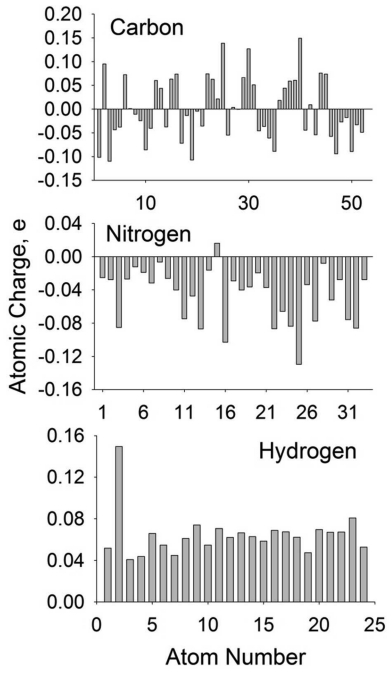

Figure 10. Atomic charges localized on carbon, nitrogen, and hydrogen atoms of system III. The charges are defined according to the Hirshfeld scheme and are given in electron units. The calculation is performed for the minimum geometry obtained at the wB97xd/6-311+G(d) level of theory. The atom numbers are the default values assigned during the computation. They do not reflect a particular order in the chemical structure.

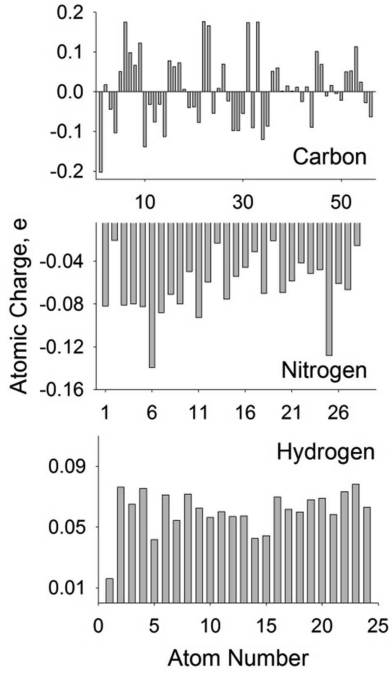

Figure 11. Atomic charges localized on carbon, nitrogen, and hydrogen atoms of system IV. The charges are defined according to the Hirshfeld scheme and are given in electron units. The calculation is performed for the minimum geometry obtained at the wB97xd/6-311+G(d) level of theory. The atom numbers are the default values assigned during the computation. They do not reflect a particular order in the chemical structure.

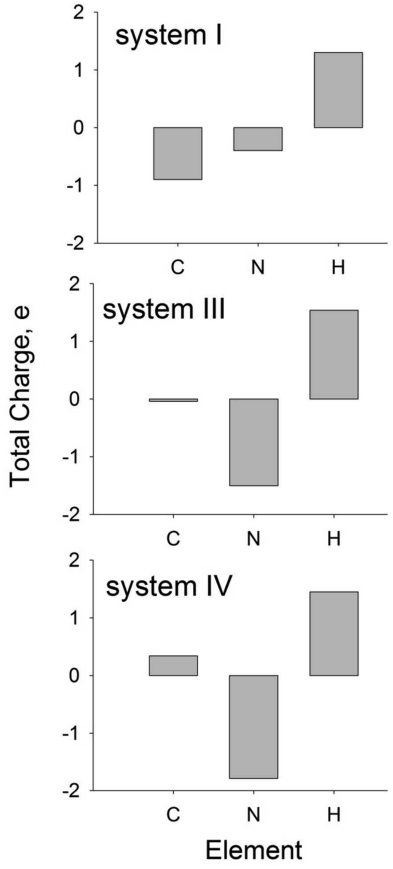

Figure 12. Total atomic charges localized on carbon, nitrogen, and hydrogen atoms of systems I, III, and IV. The charges are defined according to the Hirshfeld scheme and are given in electron units. The calculation is performed for the minimum geometry obtained at the wB97xd/6-311+G(d) level of theory.

content provided that only C−C and C−N covalent bonds are present. In turn, N−N bonds break during the very first steps of RMD, giving rise to nine- and higher-membered rings. These rings lose aromaticity and form energetically unfavorable dangling bonds. The bonds cannot be saturated in the absence of a hydrogen source. Liberated higher-energy p-electrons ionize carbon and nitrogen atoms. Thus, the second step is the destruction of carbon−nitrogen bonds, which follows destruction of nitrogen−nitrogen bonds. The decomposition of the N-doped graphene terminates at this stage, as no additional reactants are provided. The reactions proceed further in real conditions, to form simple and thermodynamically stable monomolecular products.

■ CONCLUDING REMARKS

The reported study shows that N-doped graphene can accumulate a significant amount of nitrogen atoms, as long as N−N bonds are not formed. In particular, C−N bonds remain stable at 1000 K in all graphene structures containing 1/3 of nitrogen atoms or less. Higher temperatures and structural defects can undermine the stability of the C−N bonds. In turn, the fused six-membered rings containing N−N bonds are not stable, according to our simulations. They rearrange rapidly into nine- and higher-membered rings. These are vulnerable to oxidation and other chemical reactions, which produce stable low-molecular-weight products. The simulations show that

DOI: 10.1021/jacs.5b05890
J. Am. Chem. Soc. 2015, 137, 11688−11694

electron density distribution and other electronic properties depend strongly on a specific structural pattern of N-doping.

The reported simulation results can be tested directly by chemical synthesis. Compounds with nitrogen content less than the predicted critical value will be stable, while compounds with nitrogen content larger than the critical value cannot be synthesized. Nitrogen doping constitutes an efficient means to tune, adjust, and refine mechanical and electrical properties of graphene. Nitrogen content provides a relatively straightforward route for modulating the band gap of graphene and graphene quantum dots.[33] The finite band gap of graphene quantum dots, which depends on the dot size, can be tuned further by nitrogen doping. For instance, the band gaps calculated at 0 K are equal to 3.48, 3.63, and 3.09 eV for systems I, II, and III, respectively. Nitrogen doping can be used to control the rate of nonradiative recombination of charge carriers in semiconductors, since the rate is strongly dependent on the band gap and presence of defects. Band gap opening reduces the charge recombination rate,[41] while introduction of localized states accelerate the recombination.[42] Our results provide important insights and guide engineering of N-doped graphene sheets with high nitrogen content.

■ ASSOCIATED CONTENT

Supporting Information

The Supporting Information is available free of charge on the ACS Publications website at DOI: 10.1021/jacs.5b05890.

Initial geometry of doped graphene System I, Figure 1 (TXT)
System II, Figure 1 (TXT)
System III, Figure 1 (TXT)
System IV, Figure 1 (TXT)
System V, Figure 1 (TXT)

■ AUTHOR INFORMATION

Corresponding Author

*vvchaban@gmail.com

Notes

The authors declare no competing financial interest.

■ ACKNOWLEDGMENTS

This research was in part supported by Grant CHE-1300118 from the U.S. National Science Foundation. V.V.C. is a CAPES fellow under the "Science Without Borders" program.

■ REFERENCES

(1) Cheon, J. Y.; Kim, J. H.; Kim, J. H.; Goddeti, K. C.; Park, J. Y.; Joo, S. H. *J. Am. Chem. Soc.* **2014**, *136*, 8875.
(2) Jiao, Y.; Zheng, Y.; Jaroniec, M.; Qiao, S. Z. *J. Am. Chem. Soc.* **2014**, *136*, 4394.
(3) Zhao, A. Q.; Masa, J.; Xia, W.; Maljusch, A.; Willinger, M. G.; Clavel, G.; Xie, K. P.; Schlogl, R.; Schuhmann, W.; Muhler, M. *J. Am. Chem. Soc.* **2014**, *136*, 7551.
(4) Zabet-Khosousi, A.; Zhao, L. Y.; Palova, L.; Hybertsen, M. S.; Reichman, D. R.; Pasupathy, A. N.; Flynn, G. W. *J. Am. Chem. Soc.* **2014**, *136*, 1391.
(5) Wang, H. B.; Xie, M. S.; Thia, L.; Fisher, A.; Wang, X. *J. Phys. Chem. Lett.* **2014**, *5*, 119.
(6) Mahmood, J.; Lee, E. K.; Jung, M.; Shin, D.; Jeon, I. Y.; Jung, S. M.; Choi, H. J.; Seo, J. M.; Bae, S. Y.; Sohn, S. D.; Park, N.; Oh, J. H.; Shin, H. J.; Baek, J. B. *Nat. Commun.* **2015**, *6*, 6486 DOI: 10.1038/ncomms7486.
(7) Usachov, D.; Fedorov, A.; Vilkov, O.; Senkovskiy, B.; Adamchuk, V. K.; Yashina, L. V.; Volykhov, A. A.; Farjam, M.; Verbitskiy, N. I.; Gruneis, A.; Laubschat, C.; Vyalikh, D. V. *Nano Lett.* **2014**, *14*, 4982.
(8) Li, X. W.; Zhou, J.; Wang, Q.; Kawazoe, Y.; Jena, P. *J. Phys. Chem. Lett.* **2013**, *4*, 259.
(9) Liang, H. W.; Wei, W.; Wu, Z. S.; Feng, X. L.; Mullen, K. *J. Am. Chem. Soc.* **2013**, *135*, 16002.
(10) Choi, C. H.; Lim, H. K.; Chung, M. W.; Park, J. C.; Shin, H.; Kim, H.; Woo, S. I. *J. Am. Chem. Soc.* **2014**, *136*, 9070.
(11) Chai, G. L.; Hou, Z. F.; Shu, D. J.; Ikeda, T.; Terakura, K. *J. Am. Chem. Soc.* **2014**, *136*, 13629.
(12) Zhao, L. Y.; He, R.; Zabet-Khosousi, A.; Kim, K. S.; Schiros, T.; Roth, M.; Kim, P.; Flynn, G. W.; Pinczuk, A.; Pasupathy, A. N. *Nano Lett.* **2015**, *15*, 1428.
(13) Lu, J.; Zhang, K.; Liu, X. F.; Zhang, H.; Sum, T. C.; Neto, A. H. C.; Loh, K. P. *Nat. Commun.* **2013**, *4*, 2681 DOI: 10.1038/ncomms3681.
(14) Wang, S. Y.; Zhao, X. S.; Cochell, T.; Manthiram, A. *J. Phys. Chem. Lett.* **2012**, *3*, 2164.
(15) Kovtyukhova, N. I.; Wang, Y. X.; Berkdemir, A.; Cruz-Silva, R.; Terrones, M.; Crespi, V. H.; Mallouk, T. E. *Nat. Chem.* **2014**, *6*, 957.
(16) Colherinhas, G.; Fileti, E. E.; Chaban, V. V. *J. Phys. Chem. Lett.* **2015**, *6*, 302.
(17) Zhang, X. W.; Yang, G. W. *J. Phys. Chem. C* **2009**, *113*, 4662.
(18) Ma, L. A.; Hu, H.; Zhu, L. Y.; Wang, J. L. *J. Phys. Chem. C* **2011**, *115*, 6195.
(19) Tam, T. V.; Trung, N. B.; Kim, H. R.; Chung, J. S.; Choi, W. M. *Sens. Actuators, B* **2014**, *202*, 568.
(20) Zhao, Y.; Truhlar, D. G. *J. Phys. Chem. C* **2008**, *112*, 4061.
(21) Colherinhas, G.; Fileti, E. E.; Chaban, V. V. *Phys. Chem. Chem. Phys.* **2015**, *17*, 17413.
(22) Hyeon-Deuk, K.; Prezhdo, O. V. *ACS Nano* **2012**, *6*, 1239.
(23) Dai, Y. Q.; Long, H.; Wang, X. T.; Wang, Y. M.; Gu, Q.; Jiang, W.; Wang, Y. C.; Li, C. C.; Zeng, T. H.; Sun, Y. M.; Zeng, J. *Part Part Syst. Char* **2014**, *31*, 597.
(24) Lee, A. J.; Ensign, A. A.; Krauss, T. D.; Bren, K. L. *J. Am. Chem. Soc.* **2010**, *132*, 1752.
(25) Long, R.; Dai, Y.; Huang, B. B. *J. Phys. Chem. Lett.* **2013**, *4*, 2223.
(26) Novoselov, K. S.; Geim, A. K.; Morozov, S. V.; Jiang, D.; Katsnelson, M. I.; Grigorieva, I. V.; Dubonos, S. V.; Firsov, A. A. *Nature* **2005**, *438*, 197.
(27) Li, X. L.; Wang, H. L.; Robinson, J. T.; Sanchez, H.; Diankov, G.; Dai, H. J. *J. Am. Chem. Soc.* **2009**, *131*, 15939.
(28) Wang, H. B.; Maiyalagan, T.; Wang, X. *ACS Catal.* **2012**, *2*, 781.
(29) Hong, G.; Wu, Q. H.; Wang, C. D.; Ren, J. G.; Xu, T. T.; Zhang, W. J.; Lee, S. T. *Appl. Phys. Lett.* **2013**, *102*, 051610.
(30) Yen, H. F.; Horng, Y. Y.; Hu, M. S.; Yang, W. H.; Wen, J. R.; Ganguly, A.; Tai, Y.; Chen, K. H.; Chen, L. C. *Carbon* **2015**, *82*, 124.
(31) Lawlor, J. A.; Ferreira, M. S. *Beilstein J. Nanotechnol.* **2014**, *5*, 1210.
(32) Liu, H. T.; Liu, Y. Q.; Zhu, D. B. *J. Mater. Chem.* **2011**, *21*, 3335.
(33) Deifallah, M.; McMillan, P. F.; Cora, F. *J. Phys. Chem. C* **2008**, *112*, 5447.
(34) Wei, X. L.; Fang, H.; Wang, R. Z.; Chen, Y. P.; Zhong, J. X. *Appl. Phys. Lett.* **2011**, *99*, 012107.
(35) Lherbier, A.; Blase, X.; Niquet, Y. M.; Triozon, F.; Roche, S. *Phys. Rev. Lett.* **2008**, *101*, 036808.
(36) Chenoweth, K.; van Duin, A. C. T.; Goddard, W. A. *J. Phys. Chem. A* **2008**, *112*, 1040.
(37) van Duin, A. C. T.; Dasgupta, S.; Lorant, F.; Goddard, W. A. *J. Phys. Chem. A* **2001**, *105*, 9396.
(38) Han, S. S.; Kang, J. K.; Lee, H. M.; van Duin, A. C. T.; Goddard, W. A. *J. Chem. Phys.* **2005**, *123*, 114703.
(39) Chai, J. D.; Head-Gordon, M. *Phys. Chem. Chem. Phys.* **2008**, *10*, 6615.
(40) Chaban, V. V.; Fileti, E. E.; Prezhdo, O. V. *J. Phys. Chem. Lett.* **2015**, *6*, 913.
(41) Nelson, T. R.; Prezhdo, O. V. *J. Am. Chem. Soc.* **2013**, *135*, 3702.
(42) Habenicht, B. F.; Prezhdo, O. V. *Phys. Rev. Lett.* **2008**, *100*, 197402.

DOI: 10.1021/jacs.5b05890
J. Am. Chem. Soc. 2015, 137, 11688−11694